NUKLEONIKA 2015;60(1):161−169
doi: 10.1515/nuka-2015-0002

ORIGINAL PAPER

DE GRUYTER
OPEN

Modelling of a passive autocatalytic hydrogen recombiner – a parametric study

Antoni Rożeń

Abstract. Operation of a passive autocatalytic hydrogen recombiner (PAR) has been investigated by means of computational fluid dynamics methods (CFD). The recombiner is a self-active and self-adaptive device used to remove hydrogen from safety containments of light water nuclear reactors (LWR) by means of a highly exothermic reaction with oxygen at the surface of a platinum or palladium catalyst. Different turbulence models (k-ω, k-ε, intermittency, RSM) were applied in numerical simulations of: gas flow, heat and mass transport and chemical surface reactions occurring in PAR. Turbulence was found to improve mixing and mass transfer and increase hydrogen recombination rate for high gas flow rates. At low gas flow rates, simulation results converged to those obtained for the limiting case of laminar flow. The large eddy simulation technique (LES) was used to select the best RANS (Reynolds average stress) model. Comparison of simulation results obtained for two- and three-dimensional computational grids showed that heat and mass transfer occurring in PAR were virtually two-dimensional processes. The effect of hydrogen thermal diffusion was also discussed in the context of possible hydrogen ignition inside the recombiner.

Key words: CFD • hydrogen • large eddy simulation • catalytic recombiner • turbulence

A. Rożeń
Faculty of Chemical and Process Engineering,
Warsaw University of Technology,
1 Waryńskiego Str., 00-645 Warsaw, Poland,
Tel.: +48 22 234 6435, Fax: +48 22 825 1440,
E-mail: a.rozen@ichip.pw.edu.pl

Received: 14 August 2014
Accepted: 27 November 2014

Introduction

Hydrogen, generated in a light water nuclear reactor due to radiolysis and reaction of water with zirconium claddings, accumulates in the cooling system and in the reactor safety containment. This can lead to a local increase of hydrogen concentration above its flammability limit, accidental hydrogen ignition and possible flame propagation in the reactor safety containment [1, 2]. Different active and passive methods are used in nuclear power plants to mitigate the risk of uncontrolled hydrogen ignition, e.g.: controlled ignition, catalytic recombination, forced and natural gas circulation, injection of neutral gas or venting of the safety containment [1]. Catalytic recombination of hydrogen with oxygen is a passive method, which is conducted in passive autocatalytic recombiners (PAR) consisting of a system of metal plates, grids or a granular bed covered by platinum or palladium catalysts [3]. Hydrogen and oxygen are adsorbed on the catalyst surface, and after the catalyst ignition they react producing water, which is then desorbed into the gas phase. The reaction heat produces natural convection flow through channels between the catalyst plates or bed, exhausting humid hydrogen depleted gas and drawing into PAR fresh cold gas from below. The gas flow is additionally accelerated by draft force created in the upper chimney section of the PAR box. Consequently, processes of

heat and mass exchange between gas and the catalyst surface occur in conditions of assisting natural and forced convection. Depending on the recombiner geometry and operating conditions, gas flow inside different sections of PAR can be laminar, transient or turbulent. The change of flow regime, especially inside the catalyst section, could affect the mass and heat transfer conditions and consequently the recombination rate.

Catalytic recombination of hydrogen starts in ambient conditions and its rate increases almost proportionally to the inlet hydrogen concentration [4]. The process requires neither external power nor supervision.

Different commercial and laboratory recombiners were investigated experimentally and modelled numerically by means of CFD methods e.g. [3] and [5–9]. Gas flow inside PAR was modelled either as laminar [5, 6, 8] or as turbulent one using the k-ε model [7] and the k-ω model [3, 9]. CFD studies were conducted with simplified assumptions concerning heat transfer between PAR external walls and the atmosphere, e.g. fully adiabatic PAR operation [6]. This work is aimed at selecting the best flow model and proposing a general method for calculation of heat loss to the environment. It has been done by extensive testing of different turbulence closure hypotheses and comparing results with those obtained for the limiting case of the fully laminar flow as well as with results obtained by means of the large eddy simulations (LES) technique. Additionally, a new calculation procedure for the total heat transfer rate from PAR external walls to the surrounding gas has been formulated.

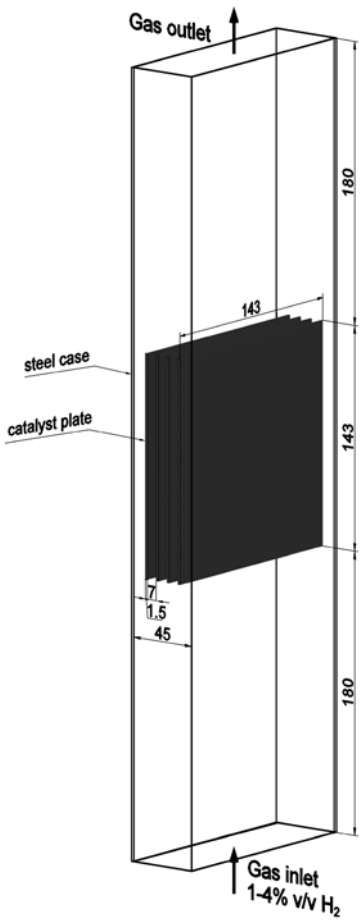

Fig. 1. Geometry of the test recombiner; dimensions are given in millimetres.

Problem description

Chemical and physical processes occurring inside PAR during its operation affect one another [5]. The exothermic hydrogen recombination reaction

$$H_2 + \tfrac{1}{2}O_2 \rightarrow H_2O \tag{1}$$

generates $\Delta H_r = 2.418 \cdot 10^5$ kJ per kmol of hydrogen [10]. This heat is released at the catalyst surface, conducted along the steel plates and PAR metal housing increasing their temperature. The reaction heat is also transferred to gas due to natural convection and irradiated from the hot catalyst surface to the PAR housing, inlet and outlet openings. Hydrogen and oxygen are transported towards the catalyst surface by molecular diffusion and convection, while steam migrates in the opposite direction. Hence, the local hydrogen recombination rate depends on: mass transfer rate, adsorption/desorption rates and surface reaction rates. These processes are directly related to: temperature, concentration gradients, physical and chemical properties (gas density and thermal conductivity, species molecular and thermal diffusivity, reaction rate constants). Differences in gas density caused by temperature and concentration gradients accelerate the upward gas flow, which in turn affects the coefficients of heat and mass transfer. All these processes form a very complicated picture of mutual dependences.

CFD software Ansys Fluent 14.5 was applied to model gas flow, heat and mass transport with chemical surface reactions proceeding in a box type recombiner consisting of: inlet, central and chimney sections as shown in Fig. 1. The central recombiner section comprises a set of four stainless steel plates covered with a platinum catalyst. Each plate is 1.5 mm thick, 0.143 m high and 0.143 m wide. The catalyst plates divide the central PAR section into vertical channels 7 and 9 mm wide. The volume of this central PAR section equals to $V = 9.202 \cdot 10^{-4}$ m^3. This geometry is similar to the geometry of a recombiner installed in REKO-3 test facility also consisting of four catalyst plates, but separated by 8.5 mm distance [11]. Experimental results obtained in this installation were used for model validation.

Model description

Gases inside autocatalytic hydrogen recombiners are far from their critical conditions. Therefore, it was assumed that a hydrogen-air-steam mixture inside PAR was an ideal gas and consequently its density ρ [kg/m^3] was estimated from the ideal gas law. The kinetic theory of gas, implemented in the Ansys Fluent code, was applied to calculate other

gas properties: thermal conductivity λ [W/(m·K)], dynamic viscosity μ [Pa·s], coefficients of molecular and thermal diffusivity of gas components D_i and $D_{T,i}$ [m²/s]. The specific heats of gas components $c_{p,i}$ [J/(kg·K)] were obtained from empirical correlations [10], while the specific heat of the gas mixture was determined as the mass average of the specific heats of all gas components. The catalyst plates and the housing of the reference PAR are made from stainless steel [11]. Hence, the average values of density, specific heat and thermal conductivity typical for this type of material were used in simulations of heat conduction: ρ_s = 7700 kg/m³, c_{ps} = 460 J/(kg·K), λ_s = 25 W/(m·K) [12].

Most heat flow generated by catalytic hydrogen recombination is removed from PAR with the effluent gas, but some part of it is transmitted to the environment through the PAR housing by natural convection and thermal radiation.

The local natural convective heat flux at vertical walls of the PAR box was estimated from

$$q_n = \bar{\alpha}_n \left(T_w - T_f\right) \tag{2}$$

The local wall temperature T_w was a variable, while the environment temperature T_f was equal to 298 K. The average convective heat coefficient $\bar{\alpha}_n$ [W/(K·m²)] was found from Churchill's correlation for the vertical flat wall [13]

$$\overline{\mathrm{Nu}}^{1/2} = 0.825 + \frac{0.387\mathrm{Ra}^{1/6}}{\left[1+\left(0.492/\mathrm{Pr}\right)^{9/16}\right]^{8/27}} \tag{3}$$

Nusselt, Rayleigh and Prandtl numbers appearing in Eq. (3) are defined as follows

$$\overline{\mathrm{Nu}} = \frac{\bar{\alpha}L}{\lambda},\quad \mathrm{Ra} = \frac{g\beta\left(\bar{T}_w - T\right)L^3}{\nu\lambda/\left(c_p\rho\right)},\quad \mathrm{Pr} = \frac{c_p\rho\nu}{\lambda} \tag{4}$$

where L is the wall height, β (1/K) is the thermal expansion coefficient and ν [m²/s] is the kinematic viscosity. Gas parameters in Eq. (4) were determined at the mean temperature

$$\bar{T} = 0.5\left(\bar{T}_w + T_f\right) \tag{5}$$

Due to the fact that the mean temperature of PAR external surfaces $\bar{T}_w$ was not known a priori, the value of the average convective heat coefficient had to be updated after reaching convergence in CFD simulations. A good start was $\bar{\alpha}$ = 6 W/(K·m²), which corresponds to $\bar{T}_w$ = 400 K. Usually no more than three corrections of the mean wall temperature were necessary to approach the constant value of $\bar{\alpha}$.

On the other hand, the local heat radiation flux between the PAR housing and the environment, could be found immediately from the Stefan–Boltzmann equation [14]

$$q_r = \varepsilon_s C_0 \left(T_w^4 - T_f^4\right), \tag{6}$$

$$C_0 = 5.669\cdot 10^{-8}\ \left[\mathrm{W}/\left(\mathrm{m}^2\mathrm{K}^4\right)\right]$$

It was assumed that the environment emissivity was equal to 1, while steel emissivity (ε_s) was set to an average value of 0.25 for polished ferritic steels [15]. Finally, superposition and integration of Eqs. (2) and (6) over PAR external walls performed in Ansys Fluent gave the cumulative rate of heat loss via the PAR housing.

Heat radiation is an even more important transport mechanism inside PAR than outside the PAR box. This is so because the catalyst plates can warm up to 800–900 K. Hence, the Ansys Fluent 'surface to surface' algorithm for calculation of surface configuration coefficients together with the Stefan–Boltzmann equation were used to determine the local values of radiative heat flux at the catalyst and steel surfaces inside PAR. Furthermore, it was assumed that the gas phase is fully transparent to heat radiation and the emissivity of washcoat platinum surface was set to an average value of 0.95 for platinum black [15].

Hydrogen should react with oxygen at the catalyst surface only without any combustion in the gas phase during normal PAR operation. Even then, according to Friedel, Rosen and Kasemo [16], at least seven reaction steps must be considered when modelling heterogeneous recombination kinetics. Fortunately, at low hydrogen concentrations in the gas phase (less than 5% v/v) and low gas humidity, Kasemo's kinetic model can be reduced to a single kinetic equation in the catalyst ignition regime [17]

$$r_{\mathrm{H_2}} = 4.695\sqrt{T}\,c_{\mathrm{H_2}}^2\,c_{\mathrm{O_2}}^{-1}\quad \left[\mathrm{kmol}/\left(\mathrm{s}\cdot\mathrm{m}^2\right)\right] \tag{7}$$

where c_i [kmol/m³] is the molar concentration of the reactants. Kasemo's model in its simplified one equation version should not be used in the case of strong oxygen deficiency. Another simple kinetic model often used in modelling catalytic hydrogen recombination is Schefer's model [18]

$$r_{\mathrm{H_2}} = 14\exp\left(\frac{-14.9\cdot 10^3}{\mathrm{RT}}\right)c_{\mathrm{H_2}}\ \left[\mathrm{kmol}/\left(\mathrm{s}\cdot\mathrm{m}^2\right)\right] \tag{8}$$

This is the first order kinetic model, which in the catalyst ignition regime predicts smaller recombination rates than Kasemo's model. Therefore, if results of CFD simulations performed using each of these kinetic models do not differ, it will mean that hydrogen recombination is limited by the rate of mass transport towards the catalyst surface rather than by the kinetics of chemical reactions.

Single step kinetic models were used to determine conditions for species and heat flux at the catalytic channel walls

$$M_i r_i = -\rho D_i \frac{\partial y_i}{\partial n}\quad \left[\mathrm{kg}/\left(\mathrm{s}\cdot\mathrm{m}^2\right)\right] \tag{9}$$

$$\Delta H_r r_{\mathrm{H_2}} = \lambda\frac{\partial T}{\partial n} - \lambda_s\frac{\partial T}{\partial n}\quad \left[\mathrm{kg}/\left(\mathrm{s}\cdot\mathrm{m}^2\right)\right] \tag{10}$$

where $\partial/\partial n$ denotes the normal variable gradient at the wall, y_i stands for mass fraction of i-th reactant and according to the reaction stoichiometry in Eq. (1)

$$r_{H_2} = \frac{1}{2} r_{O_2} = -r_{H_2O} \quad \left[\text{kmol}/(\text{s}\cdot\text{m}^2)\right] \tag{11}$$

A system of partial differential equations of: continuity, momentum, enthalpy and material balance for gas and heat conduction for the steel construction of PAR was solved numerically by means of a finite volume method implemented in the Ansys Fluent code. The following boundary conditions were applied during computations:

- inlet gas velocity $v_0 = 0.4 \div 1.6$ m/s,
- inlet gas temperature $T_0 = 298$ K and pressure $p_0 = 101\,325$ Pa,
- inlet molar fractions of hydrogen $x_{H2,0} = 0.01 \div 0.04$, nitrogen $x_{N2,0} = 0.7905(1 - x_{H2,0})$, water $x_{H2O,0} = 0$ and oxygen $x_{O2,0} = 0.2095(1 - x_{H2,0})$,
- equal mass flow rates at the inlet and the outlet of PAR,
- zero gas velocity at the catalyst plates and at PAR walls,
- species and heat flux at the catalytic channel walls given by Eqs. (9) and (10),
- zero mass flux at PAR walls,
- heat flux at the external PAR surfaces given by Eqs. (2) and (6).

The local rate of hydrogen recombination – Eqs. (7) or (8) – was implemented into the CFD code according to its definition as a surface reaction.

In order to fully account for buoyancy effects, gravitational acceleration was included in momentum, kinetic turbulent energy and turbulent dissipation transport equations. Simulations were conducted for laminar and turbulent flow conditions. Four different Reynolds average stress models (RANS) were applied:

a) k-ω model,
b) k-ε model,
c) transition shear stress model (intermittency model),
d) Reynolds stress model (RSM).

Additionally, the large eddy simulation method (LES) with Smagorinski–Lilly sub-grid turbulence model was used to calculate the velocity, temperature and concentration fields inside PAR for the highest inlet velocity $v_0 = 1.6$ m/s.

Two types of computational grids were used in CFD simulations:

- two-dimensional mesh consisting of up to 82 600 triangular and hexahedral elements,
- three-dimensional mesh consisting of up to 1 340 000 hexahedral elements

just in the central section of PAR. Better spatial resolution and consequently a finer mesh were required in near wall zones for k-ω and intermittency models and especially for the LES model ($y^+ \approx 1$) than for k-ε and RSM models ($y^+ \approx 5$). Proper mesh density in the interior regions of PAR was determined by increasing the number of mesh elements to the moment, when it had no effect on the cumulative rate of hydrogen conversion and heat transfer to the environment. Typical errors in the macroscopic mass and heat balances were kept in the range of 0.001–0.01%.

Results and discussion

There can exist different gas flow regimes inside the recombiner box. For example, when the inlet dry gas (4% v/v of hydrogen, 298 K, 10^5 Pa) enters PAR at the average velocity $\bar{v} = 1.6$ m/s, then the Reynolds number based on hydraulic diameter d_h

$$\text{Re} = \frac{\bar{v} d_h}{\nu} \tag{12}$$

is close to 7100 at the inlet. Then it drops below 1000 in the channels between the catalyst plates, while in the outlet zone the Reynolds number may increase again to 5000–6000 depending on gas temperature. In these conditions, turbulent gas motion should decline in the central PAR zone. Reducing the inlet velocity to 0.8 m/s, i.e. to the maximum inlet velocity reported for REKO-3 test facility [11], would result in a mixed flow regime in the chimney section, while reducing the inlet velocity to 0.4 or less [m/s] would result in laminar gas flow in the entire recombiner. Hence, in this parametric study, the inlet velocity was chosen in such a way as to secure turbulent flow conditions below and above the central PAR section.

CFD modelling, performed in this work, confirmed a decay of turbulent motion in the central PAR section. Figure 2 clearly shows that all tested RANS models predicted the drop of the ratio of turbulent to molecular gas viscosity (μ_t/μ) below unity in the narrow vertical channels. Turbulent motion is then gradually restored in the chimney section. It should be noted that the k-ω model predicted the slowest changes of the viscosity ratio (μ_t/μ) in the channels entrance sections (decline) and in the chimney zone (rise). On the contrary, RSM and k-ε models predicted considerably faster changes of the viscosity ratio, especially just above the catalyst plates. Shortening of transition or recirculation zones is typical for RSM and k-ε high Reynolds number models, which are usually recommended for well developed turbulence. In fact, the k-ω model is also a high Reynolds number model, but it can predict the variation of turbulence variables through the viscous sublayers all the way up to the wall. Furthermore, in the present work its version with a low Reynolds number correction for weakly developed turbulent flows was applied [19]. Finally, the four equation intermittency model predicted wide boundary laminar layers adjacent to the channel walls, but faster than the k-ω model and slower than RSM and k-ε models decay of turbulence in the channel center. The intermittency model implemented in Ansys Fluent is a modified k-ω shear-stress transport model designed to cover transition between laminar and turbulent flows [19].

Turbulence is known to radically improve mixing and mass transfer in the direction perpendicular to flow direction, e.g. normal to the wall surface. Therefore, the decay rate of turbulence in the entrance section of the narrow channels formed by the catalyst plates should affect the local recombination rate of hydrogen, provided that it is somewhat controlled by the rate of mass transfer. Figure 3 shows that the highest cumulative recombination rate of hydrogen in PAR was predicted by the k-ω model, while the

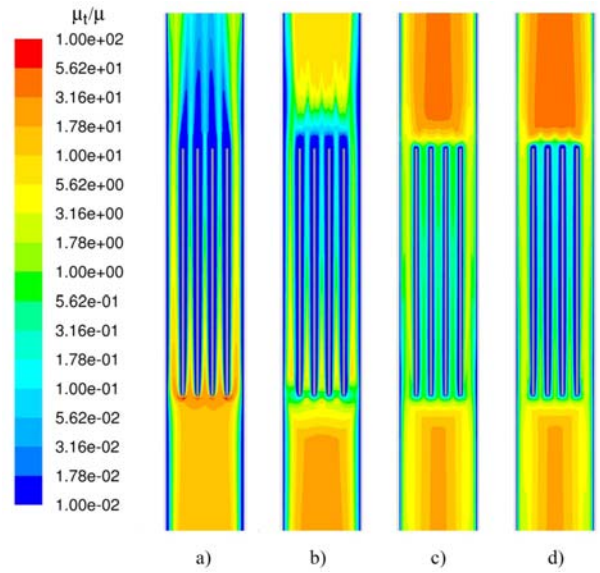

Fig. 2. Ratio of turbulent to molecular gas viscosity: k-ω model (a), intermittency model (b), RSM model (c), k-ε model (d); v_0 = 1.6 m/s, 2D mesh.

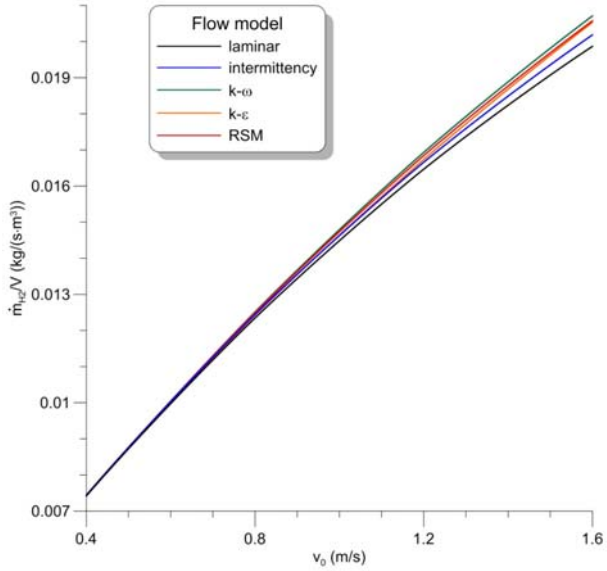

Fig. 3. Cumulative recombination rate of hydrogen per unit volume; $x_{H_2,0}$ = 0.04, 2D mesh.

lowest one was predicted in the limiting case of laminar gas flow inside the entire recombiner. RSM, k-ε and intermittency models predicted intermediate hydrogen recombination rates. Especially interesting is the case of the intermittency model, which predicted relatively slow decay of turbulence associated with quick growth of the laminar boundary sublayer after the channel entrance. These phenomena have an opposite effect on the mass transfer rate towards the catalyst surface. Consequently, the intermittency model is next to the limiting case of the laminar flow. Nevertheless, the results presented in Fig. 3 indicate that the flow laminarisation is almost complete when the gas inlet velocity approaches 0.4 m/s.

Table 1 presents cumulative hydrogen recombination rates, final hydrogen conversions and ratios of the total heat loss to surrounding, Q (W), to the total heat generated in PAR, Q_r (W), obtained for different flow models and two- and three-dimensional computational grids. The recombination rate and conversion degree were calculated by comparing hydrogen mass flow rates at the PAR inlet and outlet. Heat loss to the environment was obtained by integration of the convective and radiant heat fluxes at PAR external walls, while heat generated during hydrogen recombination was determined by integration of local heat generation by surface reactions at the catalyst walls.

It is symptomatic that the recombination rates calculated for two- and three-dimensional meshes are close to each other for all flow models. This is so because mass and heat transport in the vertical slits are virtually two-dimensional processes. Reactants are transported in two directions: normal to the catalyst surface and parallel to the gas flow. The shape of contours of the molar fraction of hydrogen (x_{H_2}) plotted in Fig. 4 for four horizontal cross-sections of PAR confirms this explanation. The highest concentration gradients of hydrogen can be observed in the direction normal to the channel walls for two cross-sections localized at 1/4 and 3/4 of the height of the catalyst plates h_c = 0.143 m. In the chimney section of PAR, these concentration fluctuations are quickly reduced by molecular and turbulent diffusion, as it can be seen for two PAR cross-sections positioned at distances 5/4 h_c and 7/4 h_c from the lower edge of the catalyst plates.

The concentration contours of hydrogen, presented in Fig. 4, were obtained for two models of turbulent flow LES and the intermittency model. The first approach is based on the observation that kinetic turbulent energy and flow anisotropy apply to large scale, geometry dependent flow motions, while the final dissipation of kinetic energy and flow isotropy are observed at smaller scales. The LES model directly resolves large turbulent eddies while sub-grid turbu-

Table 1. Hydrogen cumulative recombination rate per unit volume and final hydrogen conversion; v_0 = 1.6 m/s, $x_{H_2,0}$ = 0.04

Flow model	2D mesh			3D mesh		
	$\Delta\dot{m}_{H_2}/V$ [kg/(m³·s)]	Y_{H_2} –	Q/Q_r –	$\Delta\dot{m}_{H_2}/V$ [kg/(m³·s)]	Y_{H_2} –	Q/Q_r –
Laminar	0.01987	0.5385	0.0729	0.01989	0.5391	0.1352
k-ω	0.02071	0.5613	0.0680	0.02056	0.5572	0.1299
Intermittency	0.02019	0.5471	0.0704	0.02017	0.5468	0.1314
RSM	0.02058	0.5576	0.0625	0.02063	0.5593	0.1201
k-ε	0.02053	0.5565	0.0638	0.02064	0.5559	0.1226
LES	–	–	–	0.02012	0.5453	0.1298

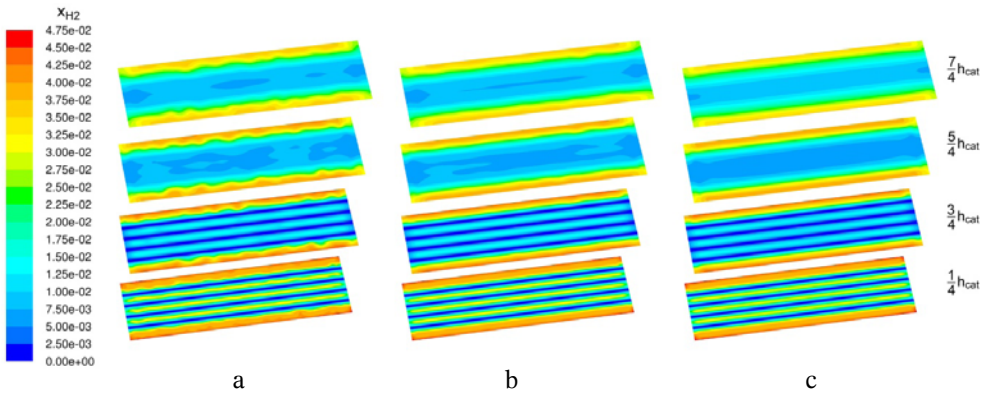

Fig. 4. Contours of the molar fraction of hydrogen at different horizontal cross-sections: LES – instantaneous (a), LES – time averaged over mean residence time (b), intermittency model (c); v_0 = 1.6 m/s, $x_{H_2,0}$ = 0.04, 3D mesh.

lent eddies are subject to an averaging procedure, e.g. sub-grid Smagorinski–Lilly technique. The LES model can be used in a wider range of the Reynolds number than RANS models and it is well suited to simulation of low Reynolds anisotropic flows characteristic for PAR. Comparison of instantaneous (Fig. 4a) and time averaged concentration contours (Fig. 4b) reveals that large eddies affect hydrogen distribution close to the side walls in the central PAR section. On the contrary, the concentration field in the inner channels, where laminar flow prevails, is practically undisturbed. The time averaged contours (Fig. 4b) are very close to those obtained with the intermittency model (Fig. 4c). This is not a surprise because according to Table 1, the intermittency model gives almost the same values of cumulative recombination rates and final hydrogen conversions as the LES model.

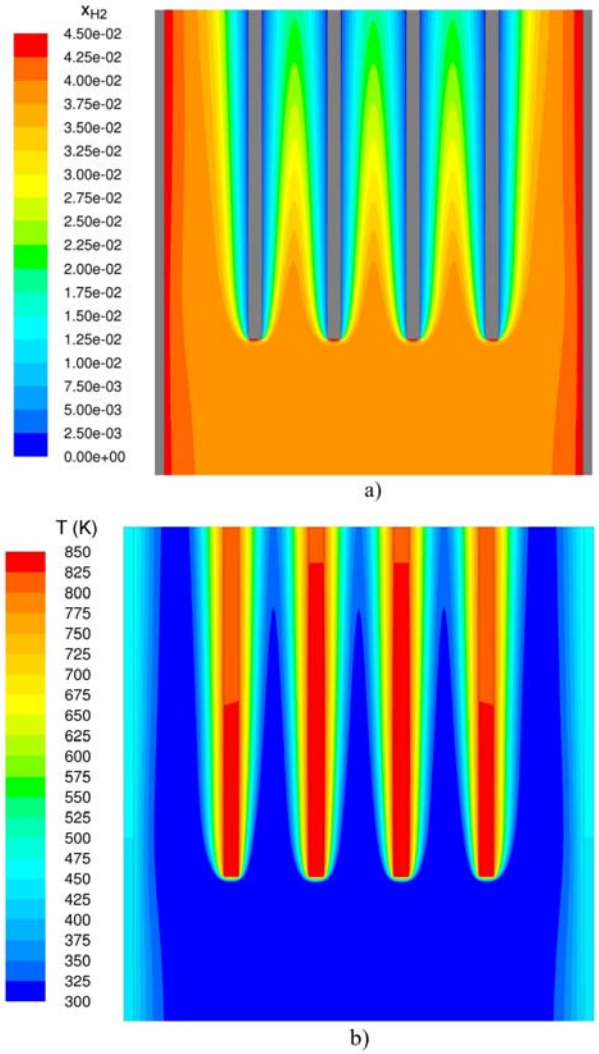

Fig. 5. Contours of the molar fraction of hydrogen (a) and temperature (b) at the entrance to the central PAR section; v_0 = 0.8 m/s, $x_{H_2,0}$ = 0.04, 2D mesh, intermittency model.

Heat generated by hydrogen recombination is transferred from the catalyst plates by: convection to the gas phase, conduction and radiation to steel elements. When the recombiner walls are not insulated, heat loss to the surrounding by natural convection and radiation occurs. The results presented in Table 1 indicate that the ratio of heat loss to the surrounding to heat generated by hydrogen recombination is approximately twice smaller for 2D than for 3D computational mesh. These results were obtained for 1 mm thick steel walls of the PAR box. Unlike a calculation of the total recombination rates of hydrogen, a correct calculation of the total heat loss requires a three-dimensional approach in CFD modelling.

Figure 5a shows another interesting phenomenon – hydrogen exceeding its inlet concentration ($x_{H_2,0}$ = 0.04). The CFD model predicts that hydrogen should migrate towards the recombiner side walls and the leading edges of the catalyst plates not covered by platinum. Such behavior can be attributed to thermal diffusion, which can be modelled with the Ansys Fluent code using the following expression for the diffusion coefficient [20]

$$D_{T,i} = -2.59 \cdot 10^{-7} T^{0.659} \left(\frac{M_i^{0.511} x_i}{\sum_{j=1}^{N} M_j^{0.511} x_j} - y_i \right) \cdot \frac{\sum_{j=1}^{N} M_j^{0.511} x_j}{\sum_{j=1}^{N} M_j^{0.489} x_j} \tag{13}$$

This form of the Soret diffusion coefficient will cause light molecules to diffuse rapidly towards hot surfaces. It should be noted that the PAR steel housing absorbs heat irradiated from the extremely hot catalyst walls. As a result, the temperature of PAR side walls

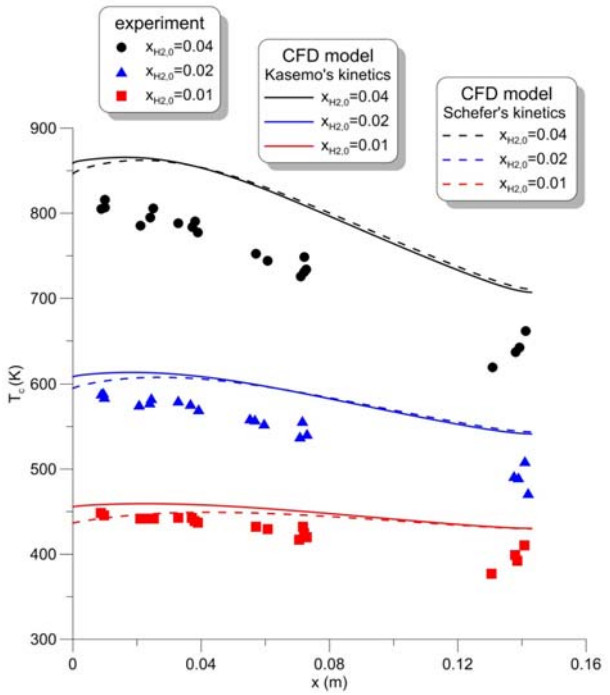

Fig. 6. Temperature at the symmetry plane of the central catalyst plate; v_0 = 0.8 m/s, 2D mesh, intermittency model.

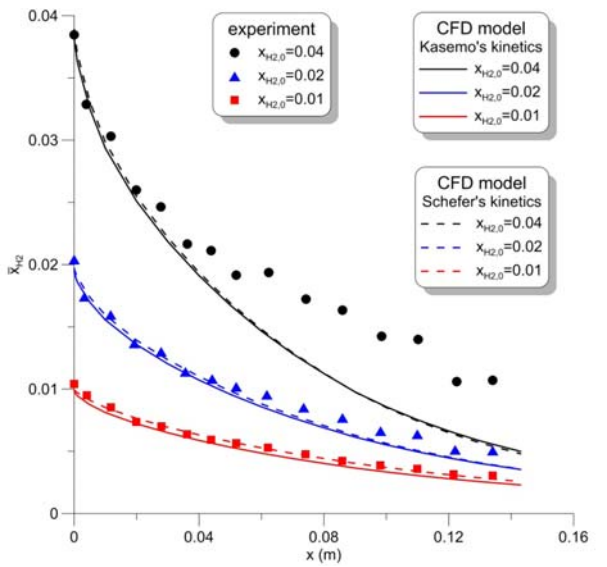

Fig. 7. Average molar fraction of hydrogen in the central PAR section; v_0 = 0.8 m/s, 2D mesh, intermittency model.

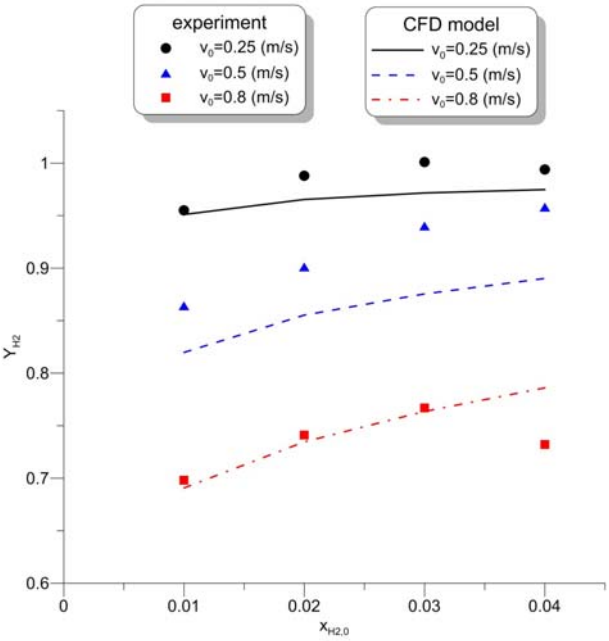

Fig. 8. Experimental and calculated (2D mesh) values of hydrogen conversion.

increases steep temperature gradient in the adjacent gas is created (Fig. 5b) and light hydrogen molecules migrate towards the side walls against concentration gradient. If confirmed experimentally, this could be a very dangerous phenomenon leading to a local overrun of the hydrogen ignition limit.

Comparison of the catalyst plate temperatures T_c [K], measured by Drinovac with thermocouples inserted in plates [11] and calculated at different distances x [m] from their lower edges, is presented in Fig. 6. The numerical simulations were conducted for two different kinetic models of hydrogen recombination: Kasemo's (Eq. (7)) and Schefer's (Eq. (8)) models. It is clear from Fig. 6 that the 'effect' of the kinetic model on the temperature profile is limited to a short distance from the plate lower edge, where the reactant transfer towards the catalyst surface is faster than the recombination reaction rate. When the concentration boundary layer grows further downstream (Fig. 5a) the process of hydrogen recombination becomes controlled by the rate of mass transfer in the direction normal to the catalyst surface. The calculated temperatures of the central catalyst plate increase strongly with the rising inlet concentration of hydrogen like the measured ones. The lower part of the catalyst plate is hotter than its upper part where the hydrogen concentration and the rate of the surface reaction are low. In most cases, the difference between the calculated and the measured temperature is not higher than 8%.

The numerical model, presented in this work, was submitted to further tests using available experimental data on hydrogen distribution inside PAR obtained by Drinovac [11], who measured hydrogen concentration in gas collected from sampling ports localized at both sides of the test recombiner and in the stream of the effluent gas; in all cases gas samples were dehumidified at molecular sieves prior to measurement. In this way, changes of hydrogen molar fraction along PAR and the final conversion degree of hydrogen could be found. Comparison of the experimental results with the results of CFD modelling is presented in Fig. 7 (concentration profiles) and in Fig. 8 (final conversion).

Concentration profiles of hydrogen, as well as temperature profiles were calculated using two different kinetic models. The concentration profiles were obtained by averaging the molar fraction of hydrogen in the central channel

$$\bar{x}_{H_2} = \frac{1}{Q_v}\iint_A x_{H_2} v\, dA \tag{14}$$

where A [m^2] is the cross-section area of gas stream, Q_v [m^3/s] is the volumetric gas flow rate and v [m/s] stands for the gas velocity. Again, analysis of the results confirms that hydrogen recombination

is diffusion controlled. A good agreement is found between the measured and calculated concentration profiles, except for the highest inlet concentration of hydrogen ($x_{H_2,0} = 0.04$) when the CFD model underestimates hydrogen molar fraction in the upper part of the channel; such a disagreement was also reported by Reinecke *et al*. (Fig. 15 in [3]).

Results presented in Fig. 8 indicate that the final conversion of hydrogen increases with decreasing inlet gas velocity. The longer the mean residence time of gas in the channels over the catalyst surface, the lower the hydrogen content in the effluent gas mixture. The CFD model and most experiments (except for two measurement points) show that increasing the inlet concentration of hydrogen also increases its final conversion. The highest differences between the calculated and measured conversion values do not exceed 7–8%. The experimentally determined final conversions are higher than the calculated ones. This may suggest that the average hydrogen concentration in the effluent gas is lower than predicted by the CFD model, despite the model's underestimation of the local hydrogen concentration in the central channel (Fig. 7).

Conclusions

The results of CFD modelling of gas flow and hydrogen catalytic recombination in the passive autocatalytic recombiner allow to conclude that a key issue in correct prediction of the cumulative recombination rate is resolution of all transport processes (momentum, heat and mass) in the central PAR section. At the entrance to this zone, gas motion changes its character from turbulent to laminar, while temperature and concentration boundary layers start to develop along the vertical catalyst surface. Four RANS models (k-ω, k-ε, intermittency and RSM) tested in this work gave completely different distributions of turbulent viscosity inside channels formed by the catalyst plates and further downstream in the chimney section. Consequently, each RANS model predicted different cumulative recombination rate of hydrogen. In order to determine which of the closure hypotheses is best suited to model PAR operation, the LES technique was applied for the first time. It turned out that the transition shear stress model also known as the four equation (kinetic energy, specific dissipation rate, flow intermittency and flow transition Reynolds number) intermittency model gave practically the same results as the LES model. Following these findings, the intermittency model was positively validated against experimental data (temperature and concentration profiles, final hydrogen conversion) available in the literature.

The new iterative procedure for calculation of the heat transfer rate from the PAR housing to the surrounding gas was implemented in CFD simulations. The procedure accounts for both convective and radiative heat transfer to the environment and allows to avoid using simplified assumptions on heat exchange.

It was confirmed by comparing the results of CFD modelling obtained for two- and three-dimensional meshes that mass transport processes occurring in the channels between the catalyst plates are virtually two-dimensional. Consequently, accurate predictions of the hydrogen removal rates are also possible in the simplified two-dimensional PAR geometry.

Finally, it was found that hydrogen can migrate inside PAR against its concentration gradient in the direction of increasing gas temperature (thermal diffusion). This phenomenon is likely to occur in the regions close to recombiner walls absorbing heat irradiated from the hot catalyst plates and may result in exceeding the hydrogen flammability limit even when the cold gas entering PAR is non-flammable.

Acknowledgments. This work was financially supported by The National Centre for Research and Development in Poland (grant no. SP/J/7/170071/12).

References

1. International Atomic Energy Agency. (2001). *Mitigation of hydrogen hazards in water cooled power reactors*. Vienna: IAEA. (IAEA-TECDOC-1196).
2. International Atomic Energy Agency. (2011). *Mitigation of hydrogen hazards in severe accidents in nuclear power plants*. Vienna: IAEA. (IAEA-TECDOC-1661).
3. Reinecke, E. A., Bentaib, A., Kelm, S., Jahn, W., Meynet, N., & Caroli, C. (2010). Open issues in the applicability of recombiner experiments and modelling to reactor simulations. *Prog. Nucl. Energy*, *52*, 136–147.
4. Fineschi, F., Bazzichi, M., & Carcassi, M. (1996). A study of the hydrogen recombination rates of catalytic recombiners and deliberate ignition. *Nucl. Eng. Des.*, *166*, 481–494.
5. Heitsch, M. (2000). Fluid dynamic analysis of a catalytic recombiner to remove hydrogen. *Nucl. Eng. Des.*, *201*, 1–10.
6. Gera, B., Sharma, P. K., & Singh, R. K. (2010). Numerical study of passive catalytic recombiner for hydrogen mitigation. *CFD Letters*, *2*, 123–136.
7. Prabhudharwadkar, D. M., & Iyer, K. N. (2011). Simulations of hydrogen mitigation in catalytic recombiner: Formulation of a CFD model. *Nucl. Eng. Des.*, *241*, 1758–1767.
8. Meynet, N., Bentaib, A., & Giovangigli, V. (2014). Impact of oxygen starvation on operation and potential gas-phase ignition of passive auto-catalytic recombiners. *Combust. Flame*, *161*, 2192–2202.
9. Klauck, M., Reinecke, E. -A., Kelm, S., Meynet, N., & Bentaib, A., & Allelein, H. -J. (2014). Passive autocatalytic recombiners operations in the presence of hydrogen and carbon monoxide: Experimental study and model development. *Nucl. Eng. Des.*, *266*, 137–147.
10. Poling, B. E., Prausnitz, J. M., & O'Connell, J. P. (2001). *The properties of gases and liquids*. Boston, USA: McGraw-Hill Co.
11. Drinovac, P. (2006). *Experimental studies on catalytic hydrogen recombiners for light water reactors*. PhD Thesis, RWTH Aachen University, Germany.
12. The European Stainless Steel Association, *Tables of technical properties of stainless steels*. Retrieved in August 2014, from http://www.euro-inox.org/technical_tables/.

13. Churchill, S. W., & Chu, H. H. S. (1975). Correlating equations for laminar and turbulent free convection from a vertical plate. *Int. J. Heat Mass Transfer*, *18*, 1323–1329.
14. Rohsenow, W. M., Hartnett, J. P., & Cho, Y. I. (1998). *Handbook of heat transfer*. New York, USA: McGraw-Hill Co.
15. Monarch Instrument. (2014). *Table of total emissivity. Metals*. Retrieved in August 2014, from http://www.monarchserver.com/TableofEmissivity.pdf.
16. Friedel, E., Rosen, A., & Kasemo, B. (1994). A laser induced fluorescence study on OH desorption from Pt in H_2O/O_2 and H_2O/H_2 mixtures. *Langmuir*, *10*, 699–708.
17. Prabhudharwadkar, D. M., Aghalayam, P. A., & Iyer, K. N. (2011). Simulations of hydrogen mitigation in catalytic recombiner: Surface chemistry modelling. *Nucl. Eng. Des.*, *241*, 1746–1757.
18. Schefer, R. W. (1982). Catalyzed combustion of H_2/air mixtures in a flat plate boundary layer: Numerical model. *Combust. Flame*, *45*, 171–190.
19. SAS IP, Inc. (2012). *Ansys Release 14.5 Theory Guide*. Canonsburg, USA.
20. SAS IP, Inc. (2012). *Ansys Release 14.5 User Guide*. Canonsburg, USA.